THE ATLANTIC-WIDE RESEARCH PROGRAMME FOR BLUEFIN TUNA (GBYP Phase 10)

SHORT-TERM CONTRACT (ICCAT GBYP 04/2021)

Design-based inference to estimate density, abundance and biomass of bluefin tuna. Reanalysis of 2010-2019 Aerial Surveys

Final Report

1 September 2021

CREEM, University of St Andrews

M Chudzinska, L Burt, D Borchers, D Miller, S Buckland

This project is co-funded by the European Union

Please cite this report as: Chudzinska et al. (2021) Design-based inference to estimate density, abundance and biomass of bluefin tuna. Reanalysis of 2010-2019 Aerial Surveys. Report number CREEM-2021-03. Provided to ICCAT, September 2021 (Unpublished).

Document control

Please consider this document as uncontrolled copy when printed.

Version	Date	Reason for issue	Prepared by	Checked by
DRAFT v1	22/07/2021	Outline of report	MC	LB SB
DRAFT v5	02/08/2021	Review by co-authors	MC	LB SB
DRAFT v7	01/09/2021	Final corrections	MC	LB SB

CREEM
Centre for Research into Ecological and Environmental Modelling

University of St Andrews

Summary

Information was required on the distribution, biomass and abundance of spawning stock (adult individuals) of bluefin tuna (BFT) in the Mediterranean Sea. Aerial surveys took place between late May and early August in years 2010-2011, 2013, 2015, 2017-2019 in four spawning regions of the Mediterranean Sea, however, spatial and temporal distribution of the surveys differed between these four regions The planes flew along pre-determined tracklines and trained observers searched for schools of tuna, recording the school size, biomass and other relevant information on the environmental conditions. A total of 146,782 km were covered on search effort during 210 days of surveys resulting in 317 sightings.

Line transect distance sampling methods (Buckland *et al.* 2001) were used to estimate tuna abundance. Two separate analyses are reported: for 2010-2015 and 2017-2019 periods due to differences in survey protocols between these two periods.
The total BFT abundance, overall surveys in 2010-2015, was 412,342 fish (95% CI 289,704 - 586,896), what translates into total biomass of 44,868,643 t kg of fish (95% CI 30,373,852 - 66,281,123). The total abundance, overall surveys in 2017-2019, was 428,874 BFT (95% CI 309,689 - 593,929), what translates into total biomass of 60,181,761 kg of fish (95% CI 43,189,143 - 83,860,066).

Introduction

To collect data in order to estimate density and abundance of bluefin tuna (BFT; *Thunnus thynnus*) in the Mediterranean Sea, a series of aerial surveys were undertaken. Surveys took place between late May and early August in years 2010-2011, 2013, 2015, 2017-2019 in four spawning regions of the Mediterranean Sea (Figure 1). Line transect distance sampling methods (Buckland *et al.* 2001) were used; the planes flew along pre-determined transects, or tracklines, and trained observers searched for animals, recording relevant information when an animal, or group of animals (here schools), was detected. In this report, data from all surveys are combined to estimate density, abundance and biomass for BFT using distance sampling analysis methods (Buckland *et al.* 2001).

Survey methods

Survey design

The exact borders and areas of the study regions have changed over the years, and the borders used in this study are depicted in Figure 1 and based on areas redefined in 2018 (see Canadas and Vazquez (2020) for details) (Table 1). The planes flew along pre-determined transects. The length and location of transects differed between regions and years (Appendix A).

Table 1. Areas [km^2] of the four surveys regions (A,C, E and G)

Region	Area [km2]
A	61837
C	51821
E	90102
G	38788

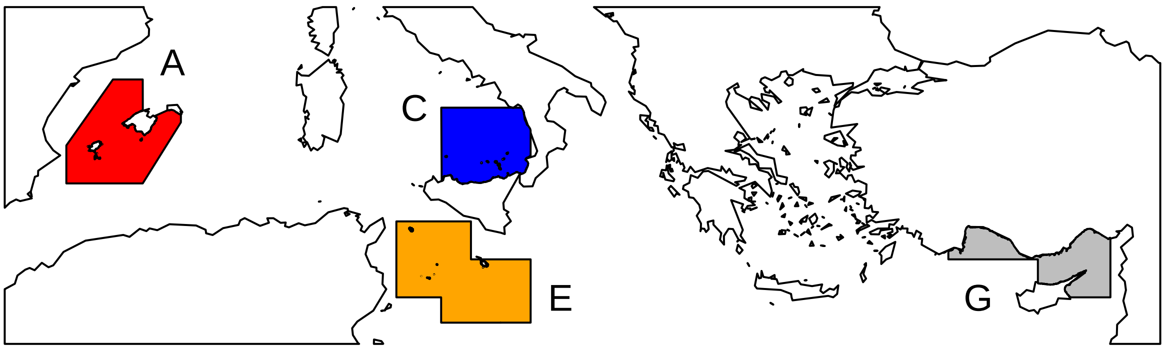

Figure 1. Location of the four survey regions: A, C, E and G.

Search protocol

Observers travelled on-board a plane; there were usually two or three observers on board: scientific and professional, see Canadas and Vazquez (2020) for details. The search protocols have changed between years, regions and companies conducting the surveys. For the majority of the surveys and detections, the observers recorded the angle to the detection relative to north, distance (or reticles) to the animal, school size, age composition, biomass as well as other information. Environmental conditions were also recorded along each transect (e.g.Beaufort sea state, visibility). See Canadas and Vazquez (2020) for description of changes in protocols as well as ICCAT GBYP reports. For the purpose of this report, only sightings of adults were taken into account (see Canadas and Vazquez (2020) for description of the distinction between adults and juveniles).

Statistical methods

Line transect distance sampling (DS) analysis methods (Buckland *et al.* 2001) were used to estimate individual density (D) as follows:

$$\hat{D} = \frac{n}{2wL\hat{p}}\hat{E}[s]$$

and abundance (N) as

$$\hat{N} = \hat{D}.A$$

where

- w is the truncation distance of perpendicular distances,
- n is the number of groups (a group can be one or more animals, like school) detected within w.
- L is total survey effort,
- $\hat{p}$ is the estimated average probability of detection within distance w of the trackline,
- $\hat{E}[s]$ is the estimated population mean school size,
- A is the area of the study region.

Details of the components of the density estimator are given below.

Survey effort

Survey effort was calculated from the start and end locations of the effort when observers were searching (on-effort).

Perpendicular distance calculation

The perpendicular distances of detections to the trackline, x, were required to estimate the probability of detection. These were calculated using the sighting angle, θ, and radial distance, r:

$$x = r.sin\theta$$

The perpendicular distances were provided prior to the analysis undertaken for the analysis of this report. Depending on the year and region, the sighting angle was estimated based on clinometer, in some cases marks on the bubble windows have been used instead (see Vazquez and Canadas (2019) for details).

Probability of detection

Two critical assumption of DS methods are that all schools on the transect centre line (i.e., at zero perpendicular distance) are detected with certainty and that distance measurements are exact. Given these assumptions, the distribution of perpendicular distances are used to model how the probability of detection decreases with increasing distance from the trackline.

The probability of detection, p, was estimated from a detection function model fitted to the observed distribution of perpendicular distances using the exact distances for fish/school. Perpendicular distances were right truncated, where required, to avoid a long tail in the detection function, as well as left truncated, where required, to account for lower detection on the transect centre line. Left truncation is a common practice for aerial surveys, due to difficulties in searching directly underneath the plane, especially when the plane does not have a bubble window. We right truncated distances based on a range of distances from 1000 to 5000 m. The choice of the final distance was based on visual inspection of fitted detection function, results of Cramer-von Mises test and distribution of probabilities of detection for each model.

Two forms of the detection function were considered: a hazard rate and a half normal.

The effect of a range of covariates was incorporated into the detection function: year (as factor, four or three levels depending on the model), region (as factor, four levels), type of airplane, company conducting surveys, type of observer, sea state, presence of bubble window, and various combination of these listed covariates. Due to unreliable assignment of bubble window and position of different observers across regions and year, bubble window and type of observer, were not included in the final process of model selection. As detectability is frequently a function not only of distance, but also school size (large schools are easier to see than small schools), then schools in the sample are likely to be larger than schools in the entire population. We therefore included school size (on a logarithmic scale) as a covariate for all models. The detected schools sizes varied between 1 and 15,000 individuals of BFT (Appendix B).

The effect of the above covariates was incorporated into the detection function model by setting the scale parameter in the model to be an exponential function of the covariates (Marques and Buckland 2004). Thus, the covariates could affect the rate at which detection probability decreases as a function of distance, but not the shape of the detection function. Adjustment terms were not included in this case.

The form that resulted in the smallest Akaike Information Criterion (AIC) was selected. Visual inspection of fitted functions, quantile-quantile plots, results of Cramer-von Mises test, estimated probability of detection and coefficient of variation were also taken into account (see Buckland *et al.* 2001 for details of detection function models and model selection methods).

Density, abundance and biomass

Detections and search effort were pooled within each survey to obtain encounter rates ($\frac{n}{L}$), and hence obtain estimates of density and abundance, by region and year.

Average estimates overall surveys (weighted by survey effort) were also obtained. To estimate biomass, estimated biomass of the schools, instead of school size, was substituted in the final models used to estimate abundance and density.

Analyses were performed in R (R Core Team, 2019) using the Distance library (Miller *et al.* 2019).

Results

Survey effort and number of detections

Across seven years, 146,782 km were covered on search effort during 210 days in the four regions resulting in 317 sightings of BFT. The search effort was longest in regions A and E which resulted in larger number of sightings (Table 2). In years 2013 and 2015 the surveys resulted in zero sightings in region G. Locations of search effort and sightings for each region and each year are shown in Appendix A. Most surveys lasted between 3-4 weeks and were conducted between late May and early July. An exceptionally late survey was conducted in region E in 2010 which finished in early August (Table 3).

Table 2. Search effort and number of sightings for each of the studied region. The presented values apply to all surveys, not only surveys used in the final models (e.g. after right or left truncation).

Region	Effort [km]	Sightings
A	41488	105
C	36966	47
E	53705	118
G	14624	47

Table 3. Temporal changes in survey effort.

Survey	From	To
A-2010	01-06	02-07
A-2011	15-06	11-07
A-2013	06-06	06-07
A-2015	01-06	11-07
A-2017	30-05	26-06
A-2018	31-05	28-06
A-2019	28-05	28-06
C-2010	05-06	29-06
C-2011	19-06	08-07

Survey	From	To
C-2013	18-06	28-06
C-2015	01-06	06-06
C-2017	30-05	14-06
C-2018	28-05	16-06
C-2019	03-06	16-06
E-2010	06-06	03-08
E-2011	13-06	29-06
E-2013	22-06	12-07
E-2015	12-06	03-07
E-2017	30-05	01-07
E-2018	31-05	23-06
E-2019	01-06	04-07
G-2010	05-06	30-06
G-2017	06-06	26-06
G-2018	30-05	14-06
G-2019	28-05	11-06

Probability of detection

Due to various differences in search protocols regarding presence of bubble windows, type of observers and differences in detection along the track centreline (Canadas and Vazquez (2020)), two separate analysis are presented: analysis for period 2010-2015 and 2017-2019 data (Appendix C). Due to no survey in 2011 and no sightings in years 2013 and 2015, region G was excluded from the analysis of 2010-2015 data. The maximum perpendicular distance for period 2010-2015 was 9850.9 m, and 19,436 m for 2017-2019, however, to avoid a long tail in the detection function, a truncation distances of 4000 and 1500 m were used respectively. We also excluded sightings within 200m of the track centreline and, for remaining sightings, subtracted 200 m (left truncation) from all distances for period 2010-2015 to account for lower detection along the track centreline. We did not use 'standard' left truncation, which would, instead, extrapolated the fitted detection function to zero distance. This resulted in 125 sightings for 2010-2015 period, and 112 for 2017-2019. Hazard-rate model including Year (as factor) was selected for 2010-2015 period. It showed better goodness of fit and lower CV around estimated abundance (see below) than the model with comparable AIC having also Company as a covariate (Table 4). Half-normal model including Company as a covariate was selected for 2017-2019 period. It showed better goodness of fit than the model with comparable AIC having Airplane as a covariate (Table 5).

Table 4. List of the covariates used for a given model ('Model', note that all models have log of school size as a covariate), key function, p values for Cramer-von Mises test, estimated average probability of detection (p), coefficient of variation (p.CV), and AICc for models fitted to 2010-2015 period. Only models which converged are presented.

Model	Key function	p value of C-vm	p	p.CV	Delta AIC
Year + Company	Hazard-rate	0.9739	0.189	0.1919	0
Year	Half-normal	0.05406	0.268	0.1115	2.148
Year + Company	Hazard-rate	0.8576	0.188	0.1139	3.26
Year	Half-normal	0.05329	0.2583	0.2105	3.313
Company	Half-normal	0.01576	0.2724	0.1131	7.428
Company	Hazard-rate	0.8137	0.1947	0.2142	8.207
Airplane	Half-normal	0.008876	0.2781	0.1126	8.659
School size only	Half-normal	0.006983	0.2846	0.1167	9.559
Airplane	Hazard-rate	0.781	0.1988	0.193	11.2
Region	Half-normal	0.007798	0.2862	0.1148	11.67

Model	Key function	p value of C-vm	p	p.CV	Delta AIC
Sea state	Half-normal	0.009971	0.282	0.1181	14.8
School size only	Hazard-rate	0.6566	0.207	0.2041	17.21
Region	Hazard-rate	0.6716	0.1793	0.233	18.24
Sea state	Hazard-rate	0.7394	0.1989	0.2153	23.92

Table 5. List of the covariates used for a given model ('Model', note that all models have log of school size as a covariate), key function, p values for Cramer-von Mises test, estimated average probability of detection (p), coefficient of variation (p.CV), and AICc for models fitted to 2017-2019 period. Only models which converged are presented.

Model	Key function	p value of C-vM	p.CV	p	Delta AIC
Airplane	Half-normal	0.5023	0.3057	0.1373	0
Company	Half-normal	0.5792	0.3024	0.136	1.19
Region	Half-normal	0.7154	0.3007	0.136	1.774
Airplane	Hazard-rate	0.02875	0.4002	0.1044	1.965
Company	Hazard-rate	0.03562	0.3951	0.1054	3.435
Region	Hazard-rate	0.04758	0.3938	0.1045	4.431
Region + Company	Half-normal	0.7737	0.3005	0.1397	5.048
Region + Company	Hazard-rate	0.04151	0.3941	0.1262	8.32
School size only	Half-normal	0.2339	0.3483	0.1202	9.044
Sea state	Half-normal	0.3578	0.3242	0.132	10.58
Sea state	Hazard-rate	0.1623	0.366	0.1227	12.2
Year	Half-normal	0.2366	0.3477	0.1211	12.86
Year	Hazard-rate	0.03456	0.4173	0.1133	20.54

The selected detection functions are shown in Figure 2.

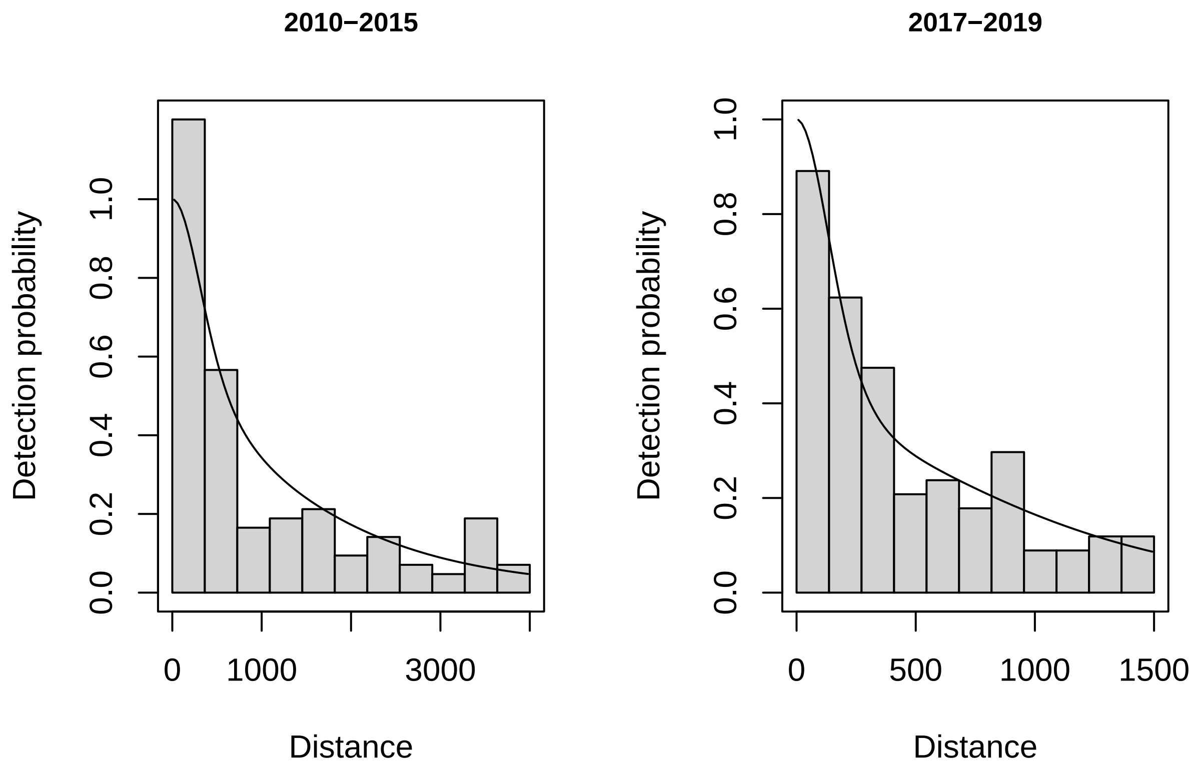

Figure 2. Average estimated detection function (black line) for the two periods overlaid onto the scaled perpendicular distance (metres) distributions.

Density, abundance and biomass

Estimates for each survey were obtained using encounter rates for each survey and applying the detection probabilities described above. The density, abundance and biomass estimates for BFT for the two periods are shown in Tables 6 - 8 and Figures 3-6.

There were large spatial and temporal differences in number of detected BFT. In early years (2010-2015), region E had the highest number of detections for most of the surveyed years. In the following years (2017-2019), the majority of detections were in region A. In the rest of the regions number of detections was low: between 2-10 regardless year. In region A, both abundance and biomass of BFT increased during the surveyed years. The remaining regions show either stable or decreasing trend. The lowest abundance and biomass was estimated for region G. The total abundance, overall surveys in 2010-2015, was 412,342 animals (95% CI 289,704 - 586,896), what translates into total biomass of 44,869 t of fish (95% CI 30,373 - 66,281). The total abundance, overall surveys in 2017-2019, was 428,874 BFT (95% CI 309,689 - 593,929), what translates into total biomass of 60,181 t of fish (95% CI 43,189 - 83,860) (Tables 6 and 7). The average size of individual fish has increased almost five-fold from 35.8 kg in 2010 to 168.6 kg in 2015 and onwards (Appendix D).

Table 6. Summary of results for period 2010-2015: detection probability (p), Search effort (km), number of schools within truncation distance (n), encounter rate (ER, schools/km) and coefficient of variation (ER.CV), individual density (N-D, fish/km^2) and coefficient of variation (N-D.CV), individual abundance (N, in thousands), coefficient of variation (N.CV) and lower (N-LCL) and upper (N-UCL) limits of the 95% confidence interval for N, expected school size (N-ES),CV (N-ES.CV), biomass (B, tonnes), CV of B (B.CV) and lower (B-LCL) and upper (B-UCL) limits of the 95% confidence interval for B, biomass density (B-D, kg of fish/km^2), coefficient of variation (B-D.CV), and expected school biomass (B-ES, kg) and CV of B-ES

(B-ES.CV).

Table 6: Table continues below

Survey	p	Effort	n	ER	ER.CV	N-D	N-D.CV	N	N.CV
A-2010	0.79	6093	8	0.0013	0.54	0.38	0.57	23.75	0.57
A-2011	0.38	7818	7	9e-04	0.38	0.21	0.44	13.17	0.44
A-2013	0.42	6667	7	0.001	0.41	0.23	0.42	13.95	0.42
A-2015	0.31	4293	6	0.0014	0.41	0.44	0.46	27.52	0.46
C-2010	0.35	8354	6	7e-04	0.44	0.09	0.61	4.54	0.61
C-2011	0.4	8684	3	3e-04	0.58	0.06	0.65	3.19	0.65
C-2013	0.48	2750	10	0.0036	0.33	1.15	0.37	59.78	0.37
C-2015	0.35	2718	2	7e-04	0.73	0.34	0.77	17.44	0.77
E-2010	0.63	12852	21	0.0016	0.38	0.54	0.55	48.51	0.55
E-2011	0.21	9980	31	0.0031	0.26	1.27	0.35	114.8	0.35
E-2013	0.14	3511	18	0.0051	0.31	0.42	0.63	37.5	0.63
E-2015	0.15	4107	6	0.0015	0.39	0.54	0.65	48.22	0.65
Total	NA	77827	125	0.0016	0.12	0.51	0.18	412.4	0.18

Table 7: Table continues below

N-LCL	N-UCL	N-ES	N_ES.CV	B	B.CV	B-LCL	B-UCL	B-D
8.31	67.87	1852	0.11	1659	0.55	591.1	4656	26.83
5.78	30.03	723.1	0.36	1392	0.43	614.3	3153	22.51
6.23	31.28	722.6	0.26	2393	0.42	1079	5304	38.69
11.62	65.17	797.3	0.1	4769	0.47	1985	11460	77.13
1.48	13.89	337.5	0.67	449.3	0.6	148.2	1362	8.67
0.98	10.35	573.7	0.37	457.1	0.62	147.7	1415	8.82
29.34	121.8	1209	0.17	7776	0.38	3733	16199	150.1
4.42	68.81	1283	0.17	2294	0.77	578.9	9088	44.26
17.37	135.4	1671	0.39	2847	0.49	1140	7110	31.6
58.85	224	677.1	0.41	7732	0.37	3798	15743	85.82
11.91	118.1	91.5	0.72	3416	0.69	991.8	11766	37.91
14.91	155.9	445.6	0.76	9691	0.6	3205	29303	107.5
289.7	587	466.8	0.26	44875	0.2	30376	66296	55.06

B-D.CV	B-ES	B-ES.CV
0.55	130.9	0.05
0.43	81.52	0.38
0.42	140.8	0.19
0.47	140.5	0.14
0.6	35.54	0.7
0.62	102.6	0.25
0.38	152.4	0.24
0.77	157.7	0.18
0.49	99.38	0.32
0.37	41.73	0.47
0.69	8.05	0.76
0.6	84.37	0.74

B-D.CV	B-ES	B-ES.CV
0.2	48.96	0.27

Table 7. Summary of results for period 2017-2019: detection probability (p), Search effort (km), number of schools within truncation distance (n), encounter rate (ER, schools/km) and coefficient of variation (ER.CV), individual density (N-D, fish/km^2) and coefficient of variation (N-D.CV), individual abundance (N, in thousands), coefficient of variation (N.CV) and lower (N-LCL) and upper (N-UCL) limits of the 95% confidence interval for N, expected school size (N-ES),CV (N-ES.CV), biomass (B, tonnes), CV of B (B.CV) and lower (B-LCL) and upper (B-UCL) limits of the 95% confidence interval for B, biomass density (B-D, kg of fish/km^2), coefficient of variation (B-D.CV), and expected school biomass (B-ES, kg) and CV of B-ES (B-ES.CV).

Table 9: Table continues below

Survey	p	Effort	n	ER	ER.CV	N-D	N-D.CV	N	N.CV
A-2017	0.17	4950	18	0.0036	0.3	0.81	0.44	49.92	0.44
A-2018	0.24	6093	24	0.0039	0.21	1.32	0.31	81.6	0.31
A-2019	0.23	5574	20	0.0036	0.24	1.21	0.38	75.02	0.38
C-2017	0.73	4791	7	0.0015	0.37	0.87	0.44	44.89	0.44
C-2018	0.58	4890	8	0.0016	0.36	0.72	0.53	37.38	0.53
C-2019	0.74	4780	4	8e-04	0.52	0.5	0.61	25.98	0.61
E-2017	0.68	6294	4	6e-04	0.5	0.49	0.54	44.1	0.54
E-2018	0.75	8713	7	8e-04	0.39	0.45	0.47	40.1	0.47
E-2019	0.88	8248	6	7e-04	0.47	0.2	0.51	17.83	0.51
G-2017	0.6	4042	4	0.001	0.49	0.08	0.72	3.17	0.72
G-2018	0.66	3969	6	0.0015	0.4	0.22	0.66	8.5	0.66
G-2019	0.38	3747	4	0.0011	0.5	0.01	0.93	0.39	0.93
Total	NA	66089	112	0.0017	0.1	0.59	0.17	428.9	0.17

Table 10: Table continues below

N-LCL	N-UCL	N-ES	N_ES.CV	B	B.CV	B-LCL	B-UCL	B-D
21.82	114.2	115.3	0.56	8001	0.45	3436	18634	129.4
45.28	147.1	239.3	0.4	13345	0.31	7352	24222	215.8
36.71	153.3	229	0.42	11548	0.38	5619	23734	186.8
19.52	103.2	1299	0.24	6749	0.43	2981	15280	130.2
13.72	101.8	771.9	0.48	5069	0.54	1846	13920	97.82
8.43	80.06	1327	0.33	3072	0.62	977.7	9652	59.28
16.38	118.7	1579	0.2	5884	0.6	1981	17483	65.31
16.63	96.71	1241	0.23	3735	0.47	1538	9067	41.45
6.96	45.68	718.6	0.09	2034	0.5	797.8	5188	22.58
0.89	11.27	147.5	0.64	287.1	0.9	62.79	1313	7.4
2.61	27.69	284.9	0.63	441.4	0.69	127.7	1525	11.38
0.08	1.85	10.82	0.53	15.82	0.94	3.29	75.95	0.41
309.7	593.9	311.6	0.22	60182	0.17	43189	83860	82.71

B-D.CV	B-ES	B-ES.CV
0.45	18.96	0.57
0.31	39.08	0.41
0.38	35.6	0.43
0.43	217	0.23
0.54	115.9	0.51
0.62	162.4	0.39

B-D.CV	B-ES	B-ES.CV
0.6	180.1	0.48
0.47	117.4	0.26
0.5	87.96	0.22
0.9	14	0.96
0.69	14.82	0.75
0.94	0.48	0.47
0.17	44.5	0.23

Table 8. Combined abundance (N, in thousands) and biomass (B, tonnes) for three regions (A, C and E) for each survey year and coefficient of variations for these estimates.

Year	N	N.CV	B	B.CV
2010	76.8	0.42	4955.57	0.36
2011	131.18	0.32	9580.98	0.31
2013	111.23	0.28	13585.08	0.28
2015	93.18	0.39	16753.71	0.39
2017	138.91	0.27	20634.78	0.28
2018	159.08	0.24	22148.51	0.24
2019	118.83	0.29	16654.31	0.3

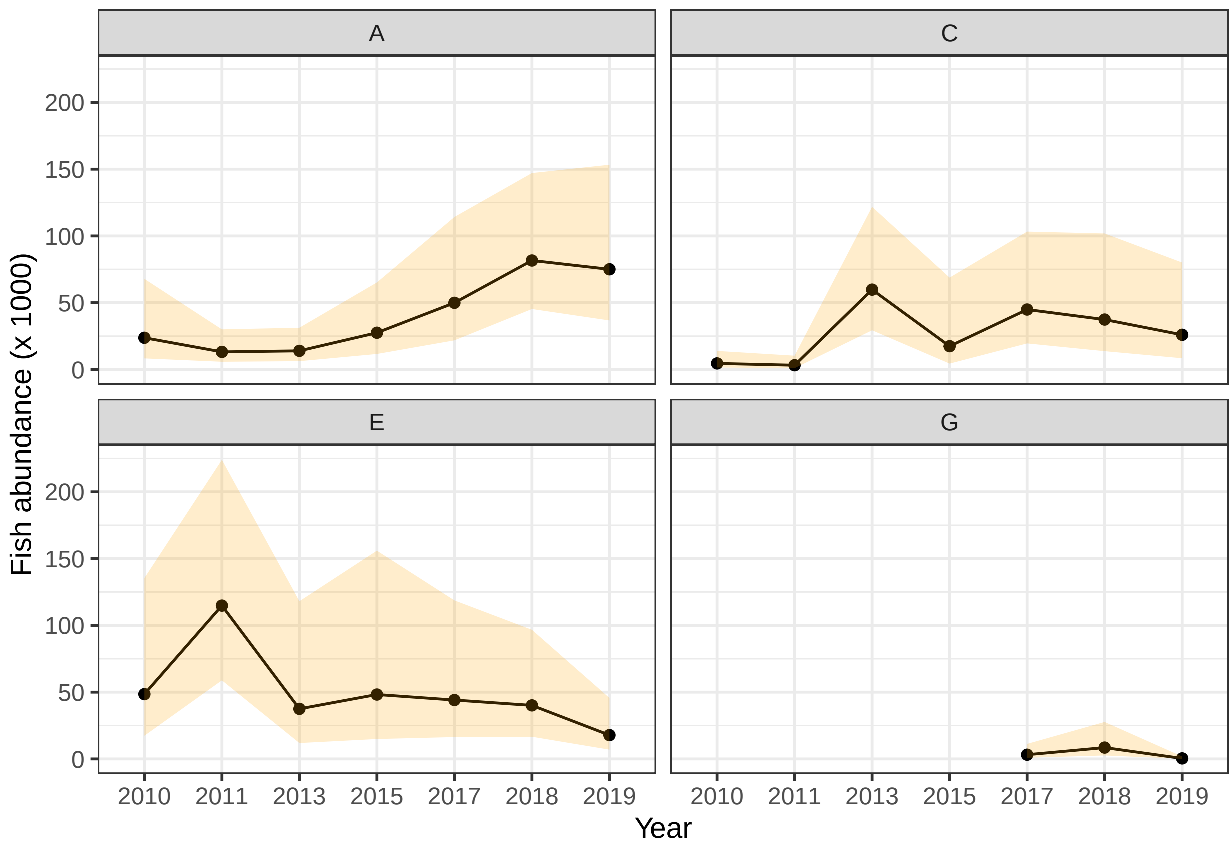

Figure 3. Estimated abundance of BFT for surveyed years and regions. Orange ribbon show upper and lower confidence limits of the 95% confidence interval.

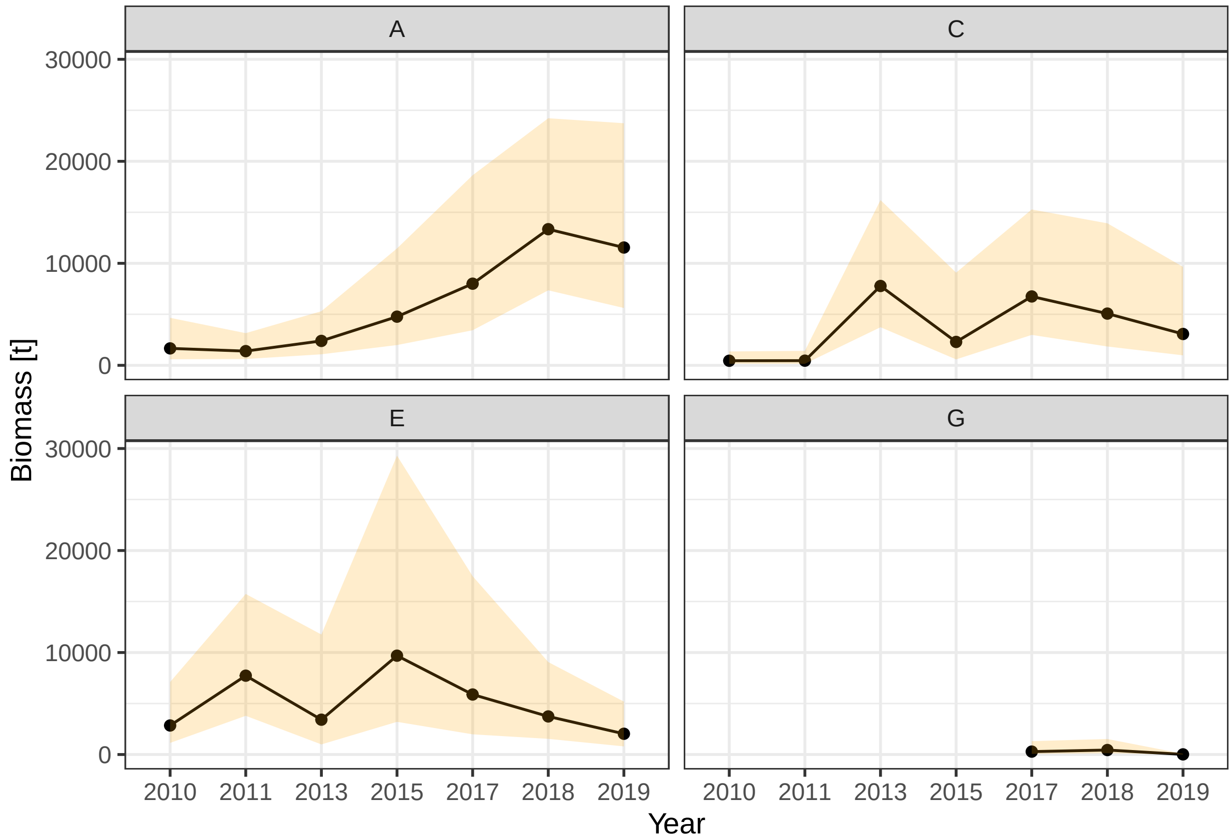

Figure 4. Estimated biomass (t) of BFT for surveyed years and regions. Orange ribbon show upper and lower confidence limits of the 95% confidence interval.

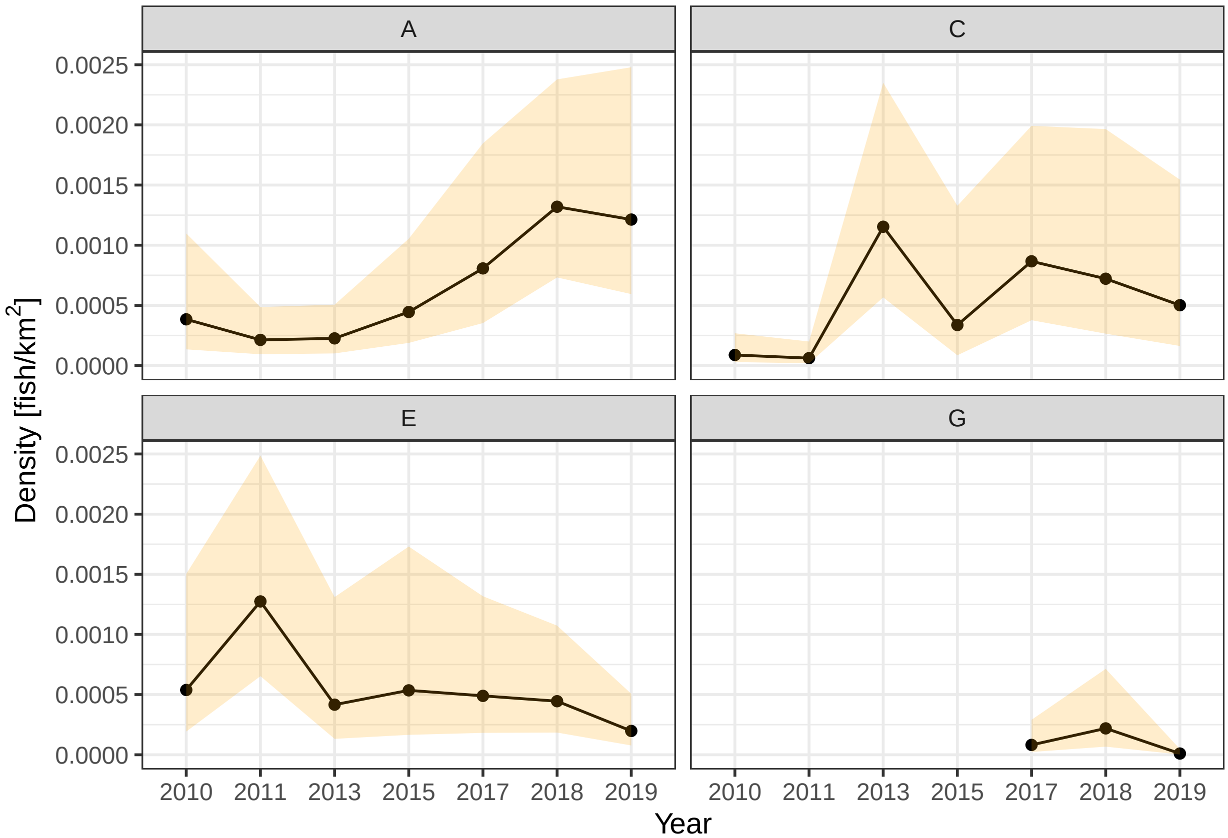

Figure 5. Estimated density (fish/km^2) of BFT for surveyed years and regions. Orange ribbon show upper and lower confidence limits of the 95% confidence interval.

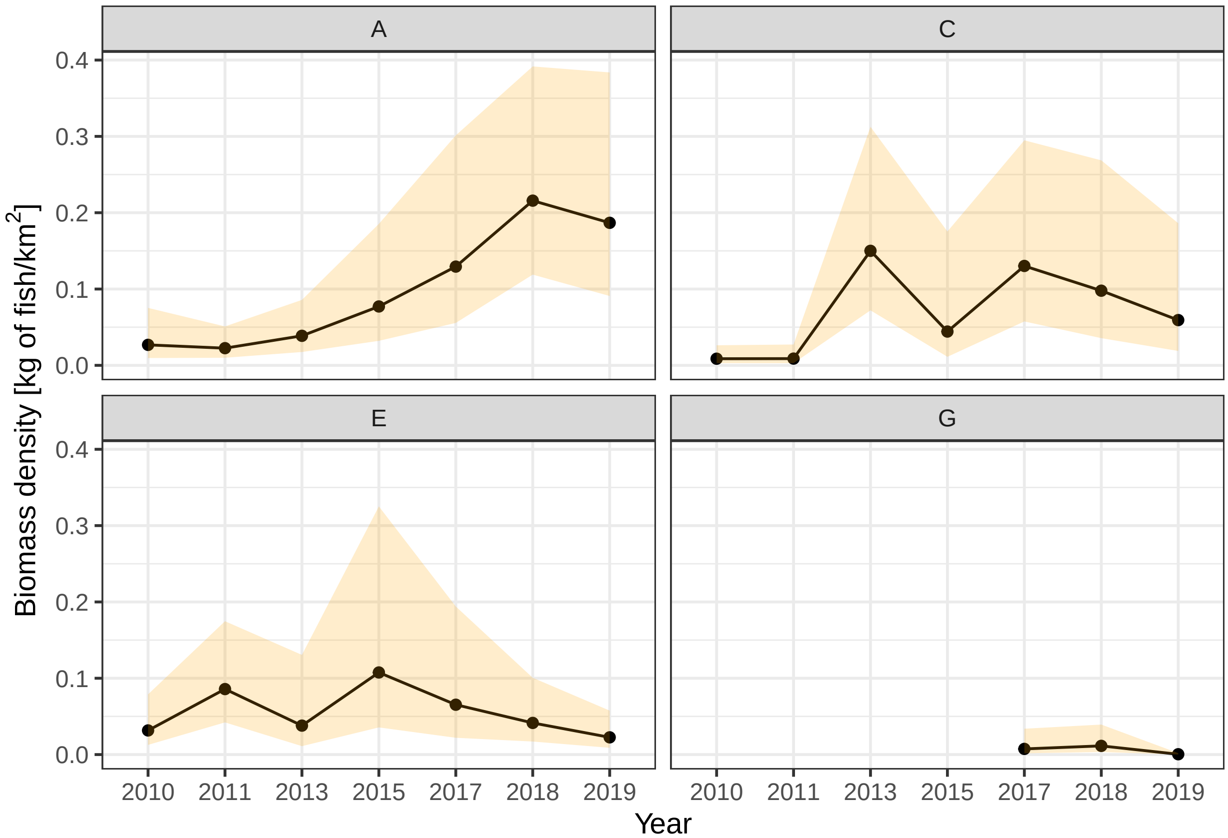

Figure 6. Estimated biomass density (kg of fish/km^2) of BFT for surveyed years and regions. Orange ribbon show upper and lower confidence limits of the 95% confidence interval.

Discussion

Abundance, density and biomass estimates by region and year, as well as overall have been reported for BFT.

Distance sampling relies on certain detection on the track centreline and if this assumption is not valid, then the estimated abundance will under-estimate true abundance; this may affect estimates of BFT albeit to differing degrees. In early years of the surveys, large number of surveys resulted in very law detectability on the track centreline. It was not possible to assign this tendency of lower detections on the trackline to a particular region, year, airplane type or company conducting the surveys. We, therefore, left truncated to 200m all the surveys in years 2010-2015 when this tendency of lower detectability was most pronounced.

Another key assumption of distance sampling methods is that perpendicular distances are exact and measured without error. Systematic bias in the measurements can result in over, or under, estimating the detection probability. A uniform protocol, where distances are estimated in the same way, both observers at the back of the plane have bubble windows is necessary. Some errors in the locations have been corrected but some errors are still be present, especially in region G (see Appendix A). If the search effort is reduced (due to corrections), the encounter rate, and hence, abundance will increase.

More analysis and research should be done to explain the differences in average fish weight across years (Appendix D). Especially whether these differences are results of a biological process or changes in search protocol. These differences between years resulted in estimates of density of biomass (kg of fish/km^2) to be even 20 times higher in later years than at the beginning of the survey. Comparable results are presented by Canadas and Vazquez (2020) (Appendix E).

The abundance estimates presented in this report are comparable to results presented in Canadas and Vazquez

(2020) for regions A, C and G (Appendix E). For region E, however, the estimates presented here are lower than in Canadas and Vazquez (2020). The mean estimates from Canadas and Vazquez (2020) are, however, within confidence intervals of the estimates presented in this report. In terms of biomass, these two estimates are comparable for all regions, except much higher estimates for year 2015 in region E in Canadas and Vazquez (2020). This may be partly the result of different 'grouping' of the data. The report presented here divides the data into two periods: 2010-2015 and 2017-2019, whereas in Canadas and Vazquez (2020), these periods are 2010-2013 and 2015-2019 respectively. The largest discrepancy between this report and Canadas and Vazquez (2020) are in expected mean fish weight. The expected mean fish weight estimated in this report varies between 44 and 195 kg (year and region dependant), whereas the same estimate from Canadas and Vazquez (2020) varied between 0.8 and 195 kg (Figure E4 in Appendix E.)

Aknowledgements

This work has been carried out under the ICCAT Atlantic-Wide Research Programme for Bluefin Tuna (GBYP), which is funded by the European Union, several ICCAT CPCs, the ICCAT Secretariat, and other entities (see https://www.iccat.int/gbyp/en/overview.asp). The content of this paper does not necessarily reflect ICCAT's point of view or that of any of the other sponsors, who carry no responsibility. In addition, it does not indicate the Commission's future policy in this area.

References

Buckland ST, Anderson DR, Burnham KP, Laake JL, Borchers DL and Thomas L (2001) Introduction to distance sampling. Oxford University Press

Canadas A, Vazquez A (2020) 2010-2019 Aerial Survey Data Re-Analysis. SHORT-TERM CONTRACT ICCAT GBYP 07/2019 Final report.

Marques FFC and Buckland ST (2004) Covariate models for the detection function. In Buckland ST, Anderson DR, Burnham KP, Laake JL, Borchers DL and Thomas L (eds) Advanced distance sampling. Oxford University Press, Oxford, UK

Miller DL, Rexstad E, Thomas L, Marshall L, Laake JL (2019) Distance Sampling in R. Journal of Statistical Software, 89(1), 1-28. doi:10.18637/jss.v089.i01 (URL: https://doi.org/10.18637/jss.v089.i01)

R Core Team (2019) R: A language and environment for statistical computing. R Foundation for Statistical Computing, Vienna, Austria. URL https://www.R-project.org/

Vazquez A, Canadas A (2019) Design of an aerial survey calibration exercise and an updated aerial surveys sighting protocol (ICCAT GBYP 08/2019) of the Atlantic-wide research programme for Bluefin Tuna (ICCAT GBYP Phase 8).

Appendix A: Locations of realised survey effort and sightings

Appendix A depicts survey effort and sightings for all four regions for each year. Only sightings for adult individuals and along on-effort transects are shown. The graphs show all transects and sightings fulfilling the above criteria and, therefore, also transects and sightings which were not taken into account in the final modelling due to e.g. truncation or missing information.

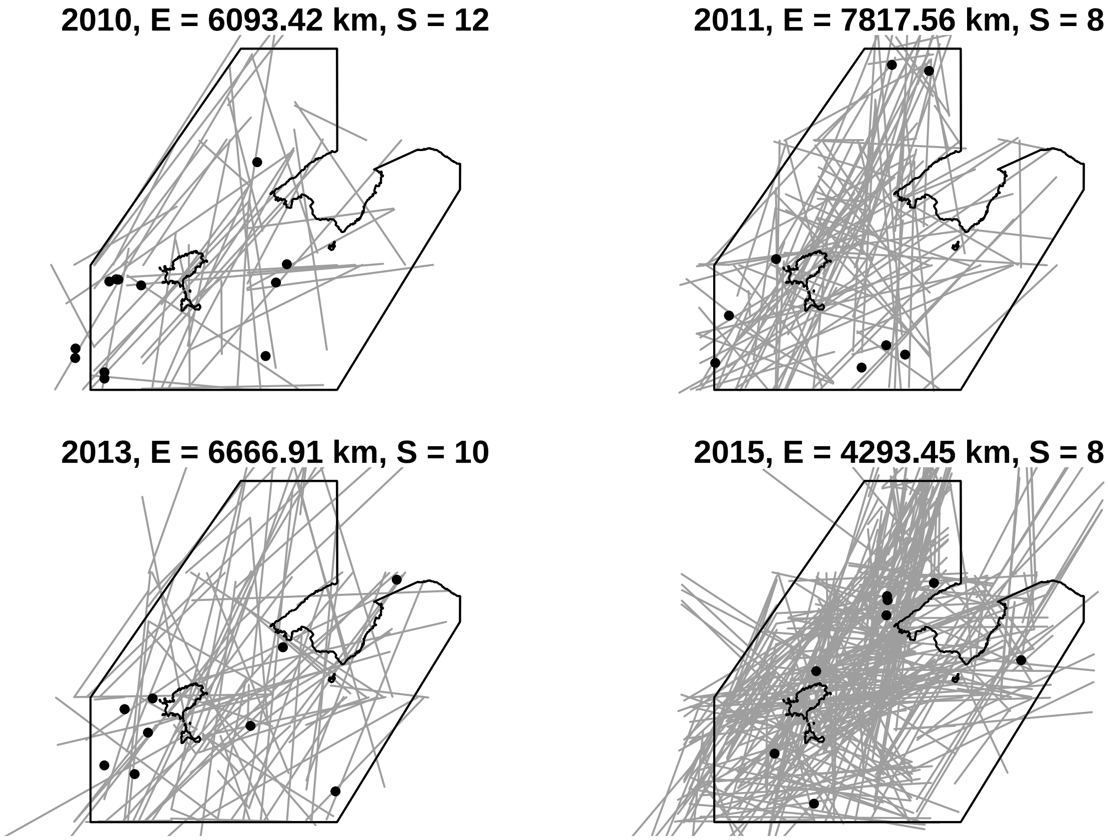

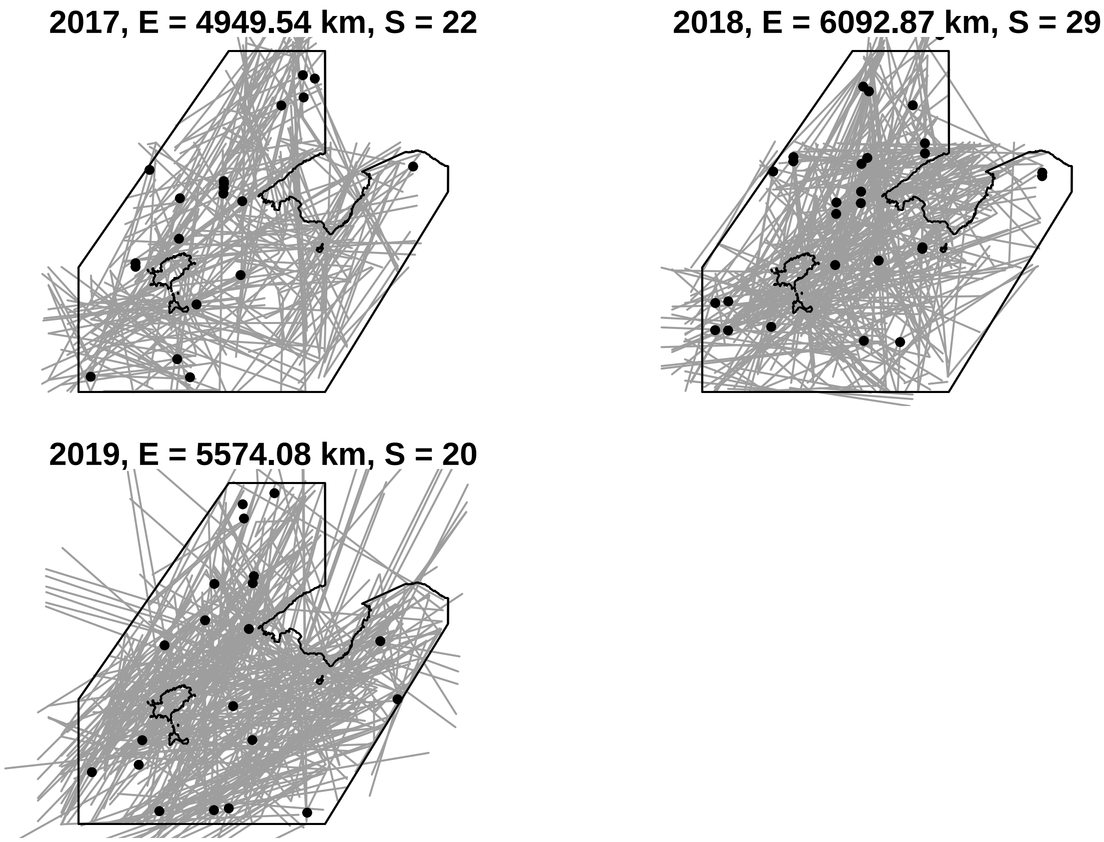

Figure A1. Location of transects in region A for each year of survey. Only on effort transects are shown. Dots represent sightings of adult individuals/schools. E indicated total length [km] of the surveyed transects in a given year and S number of sightings.

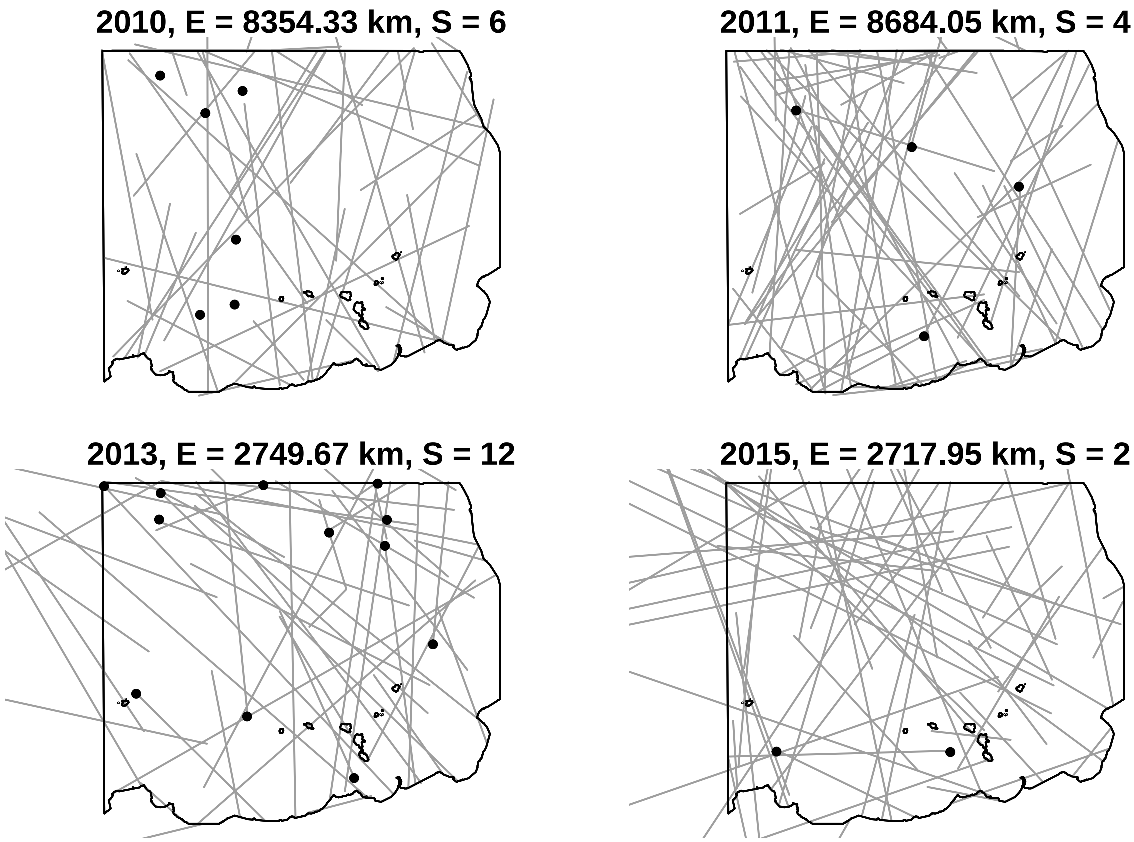
2010, E = 8354.33 km, S = 6
2011, E = 8684.05 km, S = 4
2013, E = 2749.67 km, S = 12
2015, E = 2717.95 km, S = 2

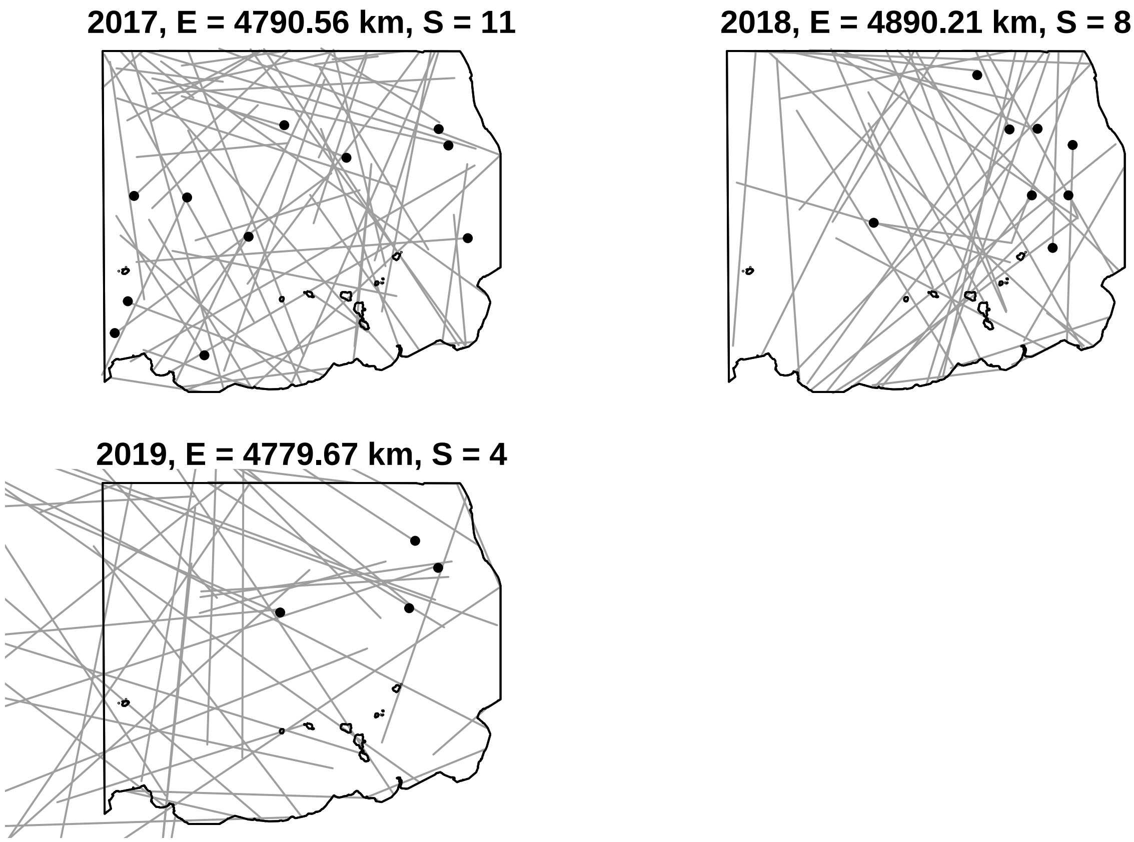

Figure A2. Location of transects in region C for each year of survey. Only on effort transects are shown. Dots represent sightings of adult individuals/schools. E indicated total length [km] of the surveyed transects in a given year and S number of sightings.

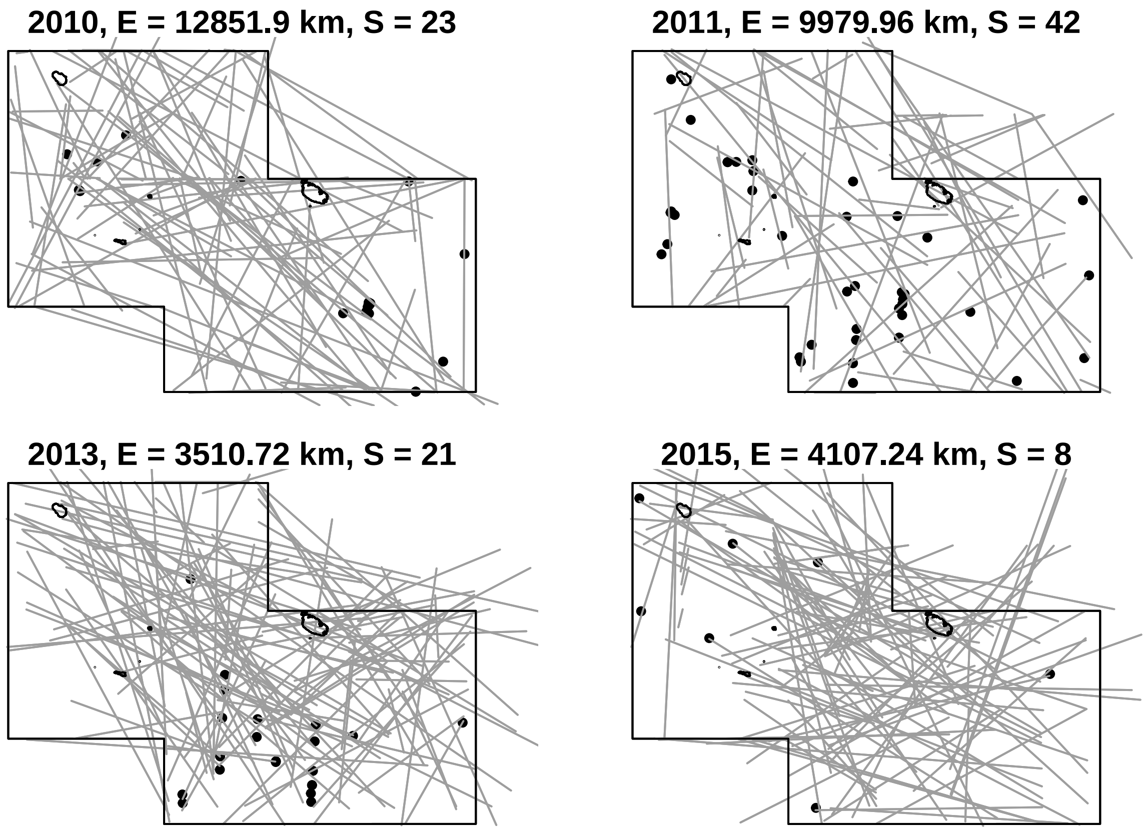
2010, E = 12851.9 km, S = 23
2011, E = 9979.96 km, S = 42
2013, E = 3510.72 km, S = 21
2015, E = 4107.24 km, S = 8

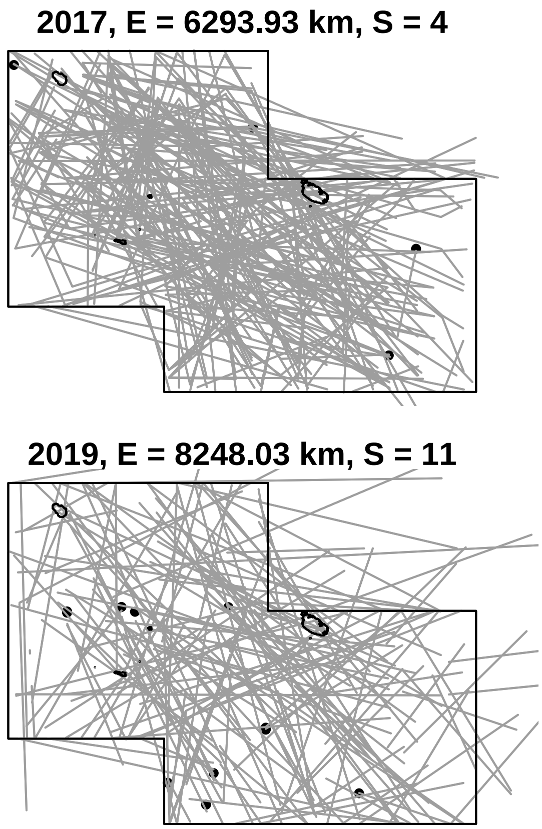

Figure A3. Location of transects in region E for each year of survey. Only on effort transects are shown. Dots represent sightings of adult individuals/schools. E indicated total length [km] of the surveyed transects in a given year and S number of sightings.

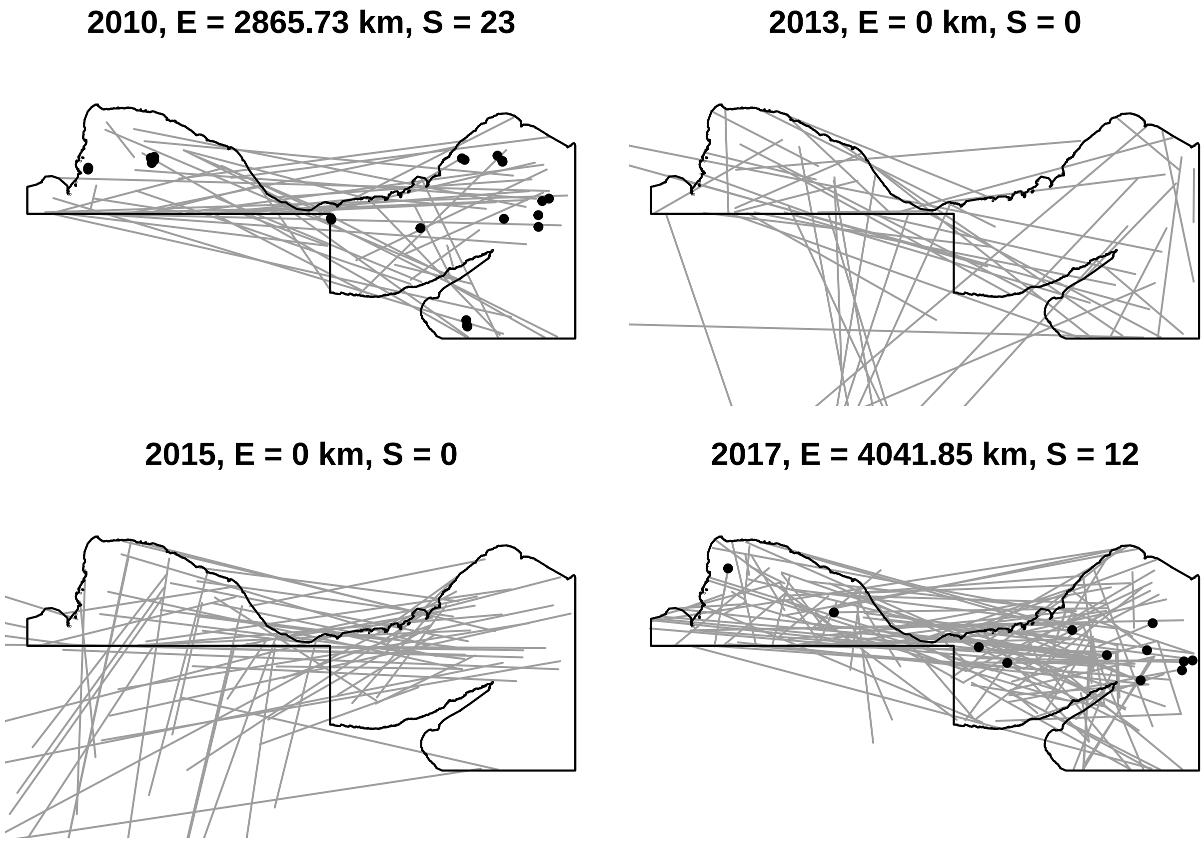
2010, E = 2865.73 km, S = 23
2013, E = 0 km, S = 0
2015, E = 0 km, S = 0
2017, E = 4041.85 km, S = 12

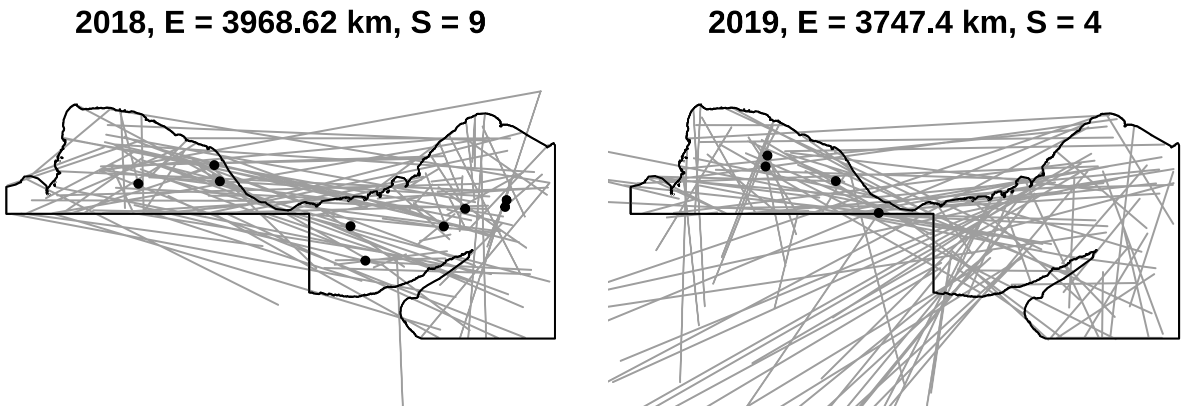

Figure A4. Location of transects in region G for each year of survey. Only on effort transects are shown. Dots represent sightings of adult individuals/schools. There was no sightings in years 2013 and 2015 and no survey in 2011. E indicated total length [km] of the surveyed transects in a given year and S number of sightings.

Appendix B: Relationship between school sizes and the detection distance.

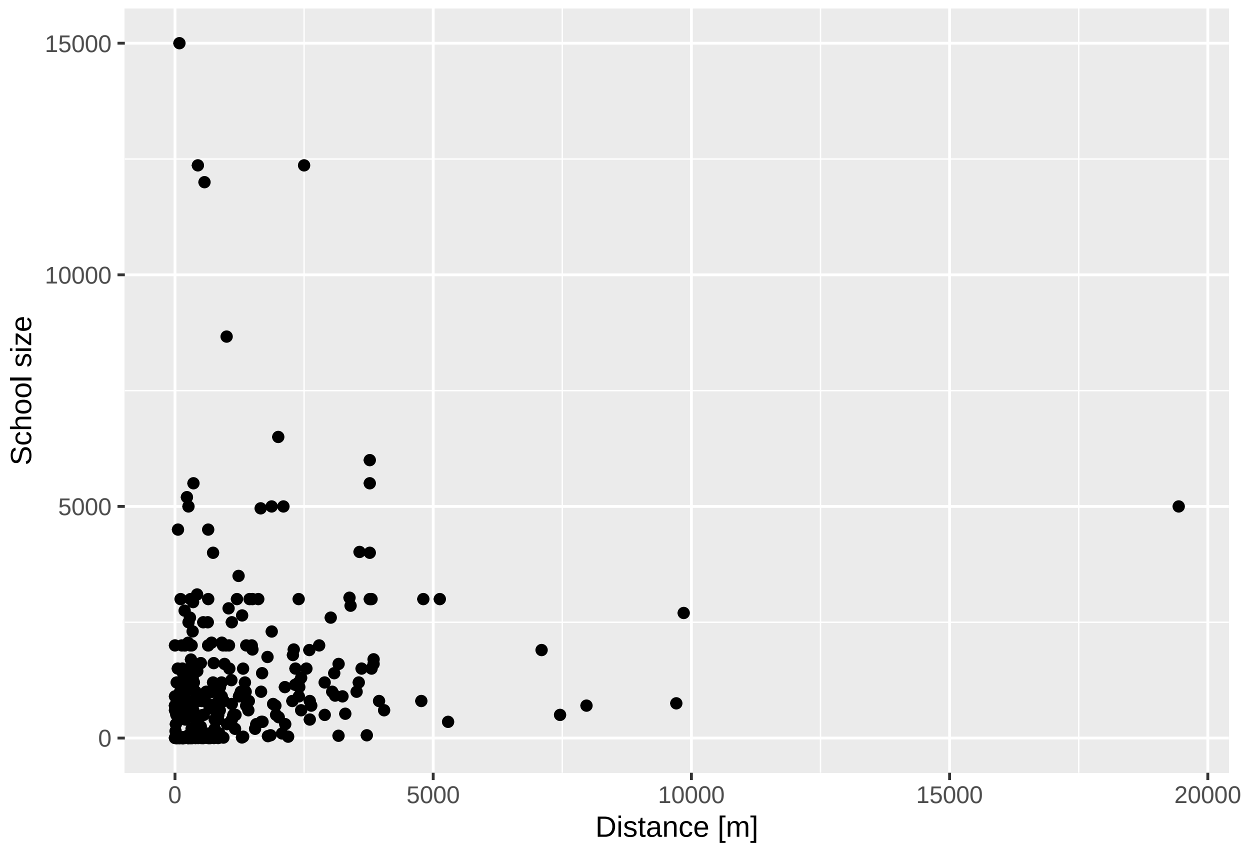

Figure B1. Relationship between school sizes and the detection distance for all detections combined.

Appendix C: Distribution of perpendicular distances between two periods

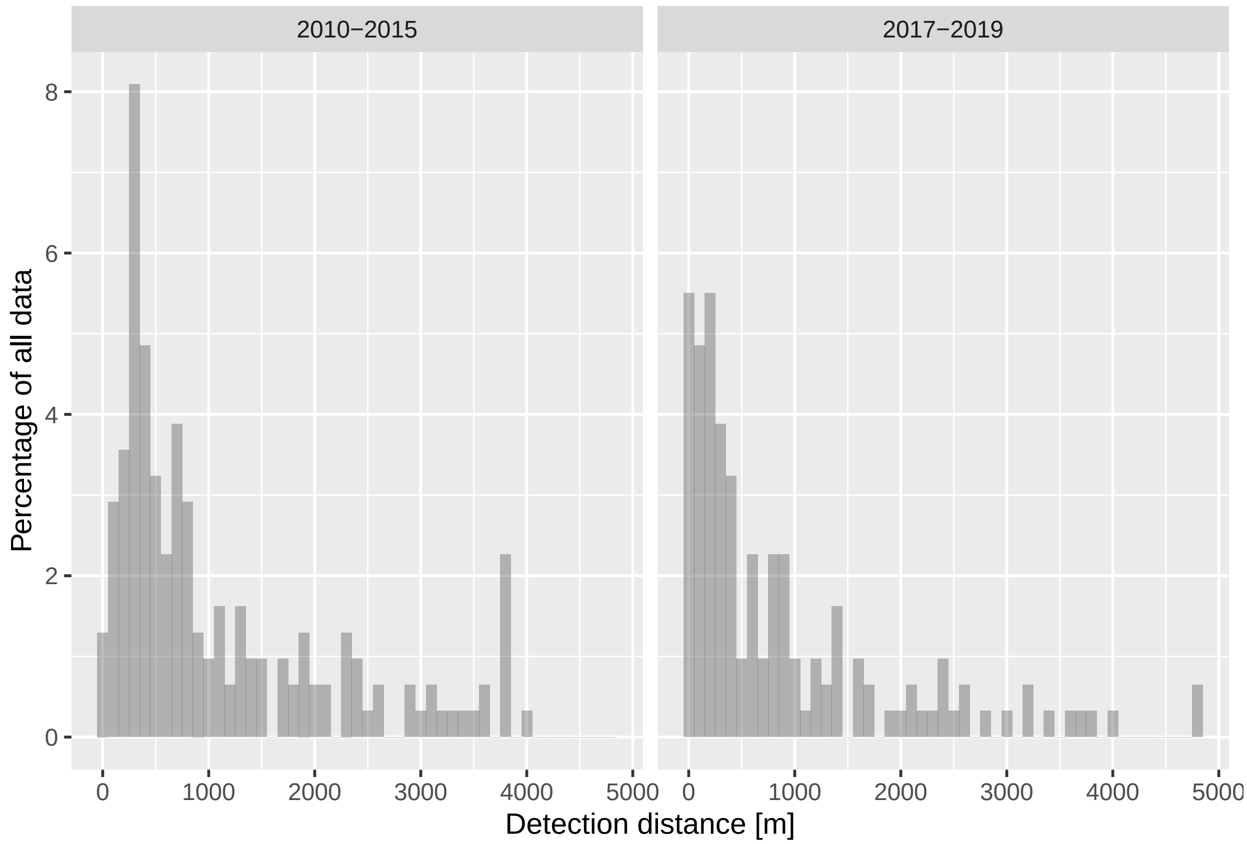

Appendix D: Temporal changes in average fish weight

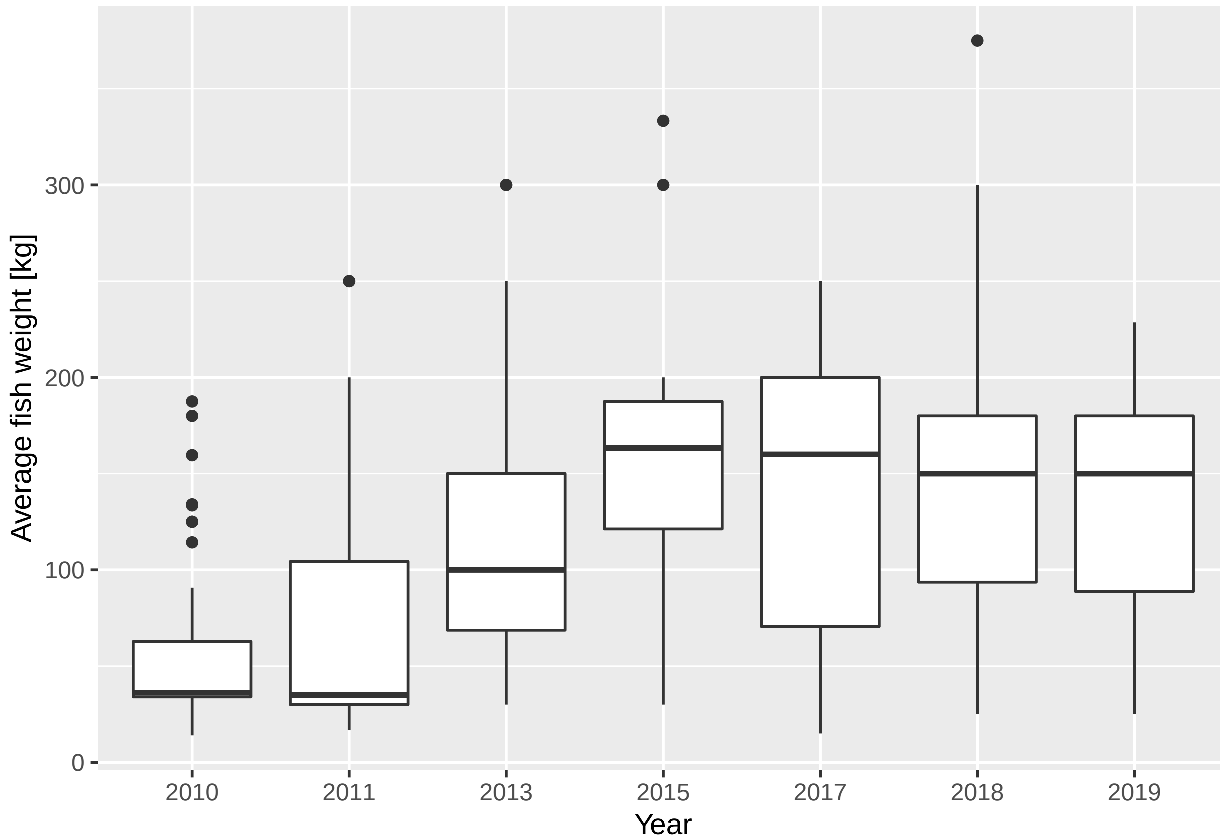

Figure 1D. Temporal changes in distribution of average fish weight. The graph is based on all 317 sightings.

Appendix E: Comparisons of abundance and biomass estimates between this report and Canadas and Vazquez (2020)

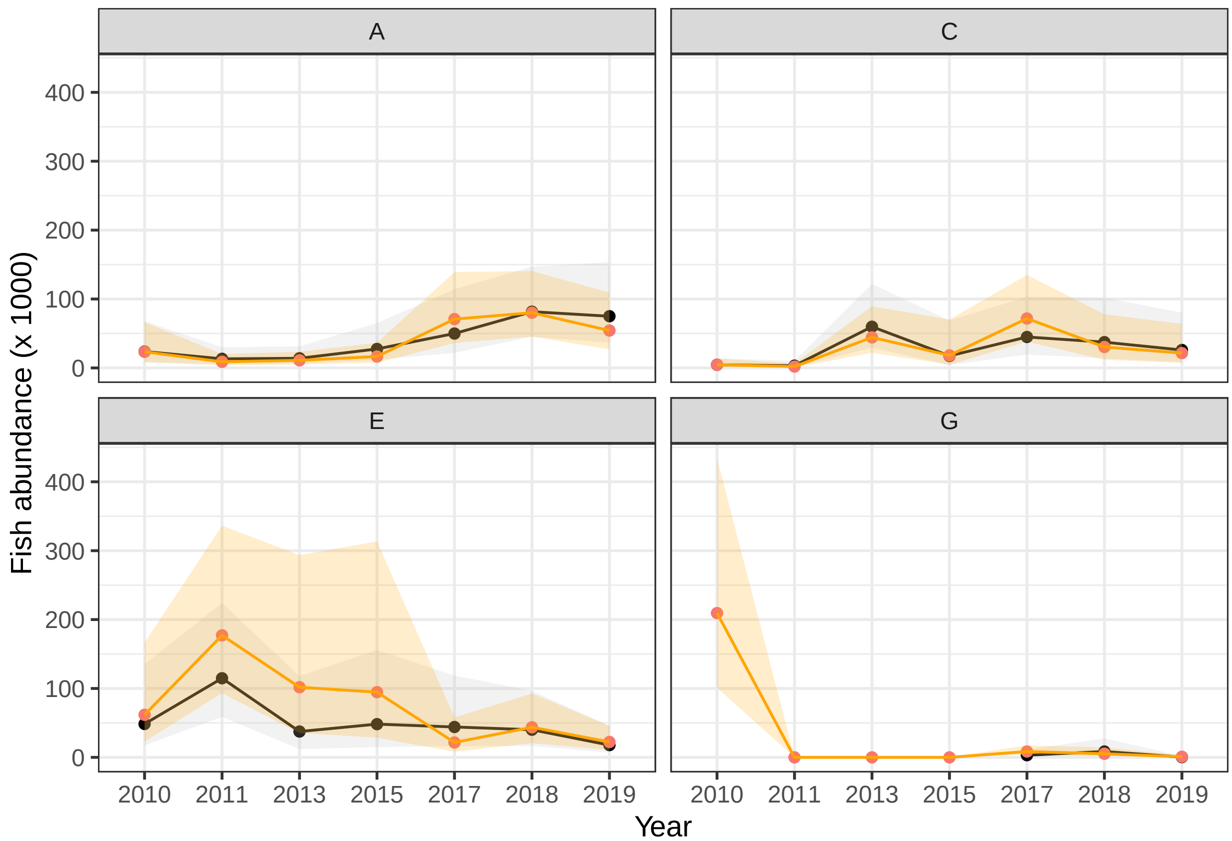

Figure E1. Comparisons of abundance between this report (black lines and grey ribbons) and Canadas and Vazquez (2020) (red lines and orange ribbons). Ribbons show upper and lower confidence limits of the 95% confidence interval.

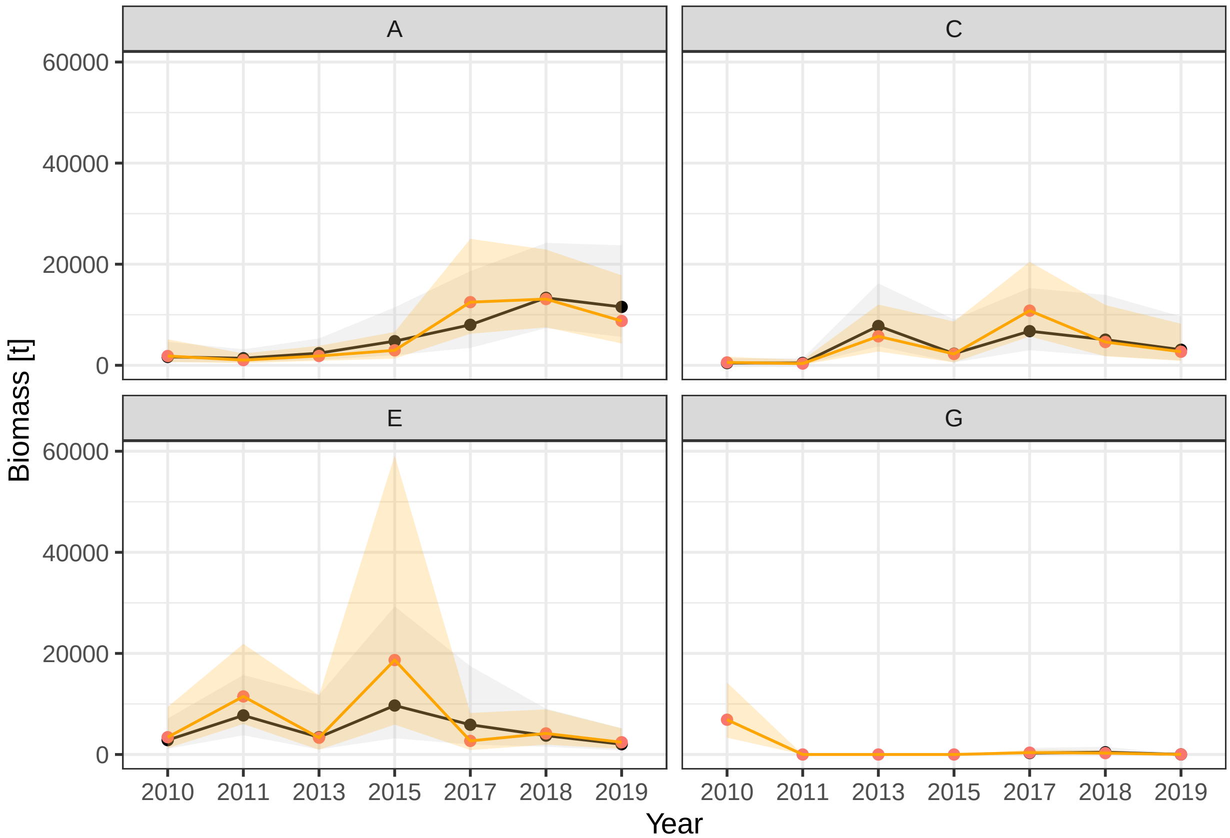

Figure E2. Comparisons of biomass (tons) between this report (black lines and grey ribbons) and Canadas and Vazquez (2020) (red lines and orange ribbons). Ribbons show upper and lower confidence limits of the 95% confidence interval.

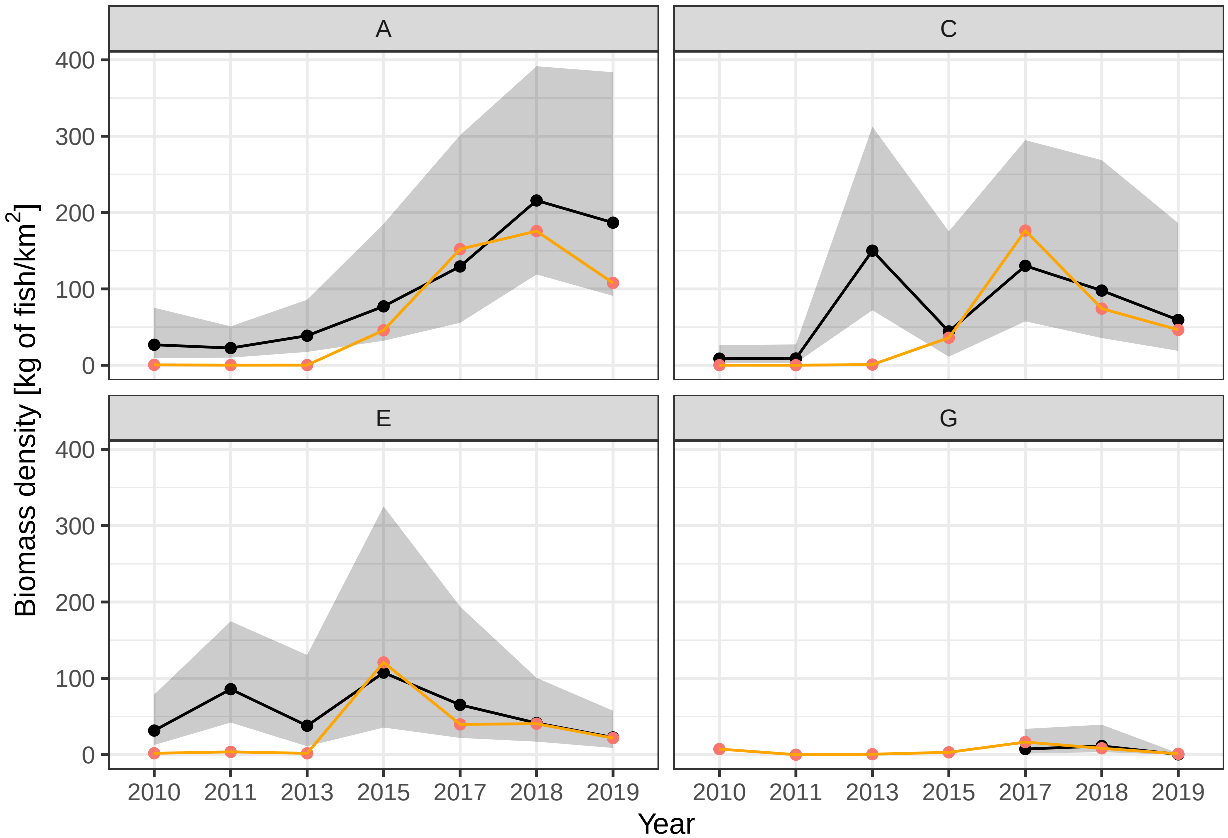

Figure E3. Comparisons of density of biomass (kg of fish/km^2) between this report (black lines and grey ribbons) and Canadas and Vazquez (2020) (red lines and orange ribbons). Ribbons show upper and lower confidence limits of the 95% confidence interval. There was no confidence intervals presented for the density of biomass in Canadas and Vazquez (2020).

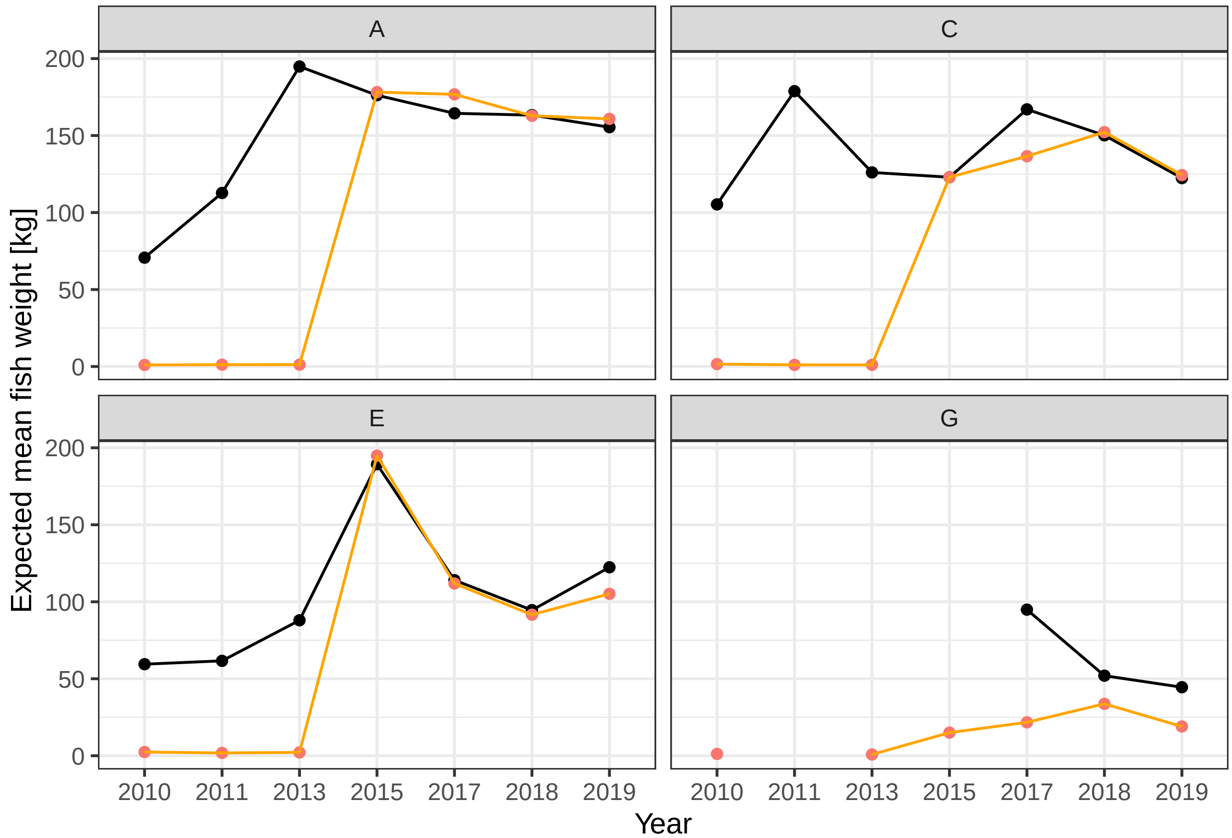

Figure E4. Comparisons of expected average fish weight (kg) between this report (black lines) and Canadas and Vazquez (2020) (orange lines). The expected average fish weight was calculated as expected school weight (kg)/expected school size.